Electronic Supplementary Information

Temperature-induced modulation of mesopore size in hierarchically porous amorphous TiO_2/ZrO_2 beads for improved dye adsorption capacity

Maryline Chee Kimling,[a] Dehong Chen[a] and Rachel A. Caruso*[a,b]

[a]*Particulate Fluids Processing Centre, School of Chemistry, The University of Melbourne, Melbourne, Victoria 3010, Australia*

[b]*CSIRO, Manufacturing Flagship, Private Bag 33, Clayton South, Victoria 3169, Australia*
**To whom correspondence should be addressed.E-mail: rcaruso@unimelb.edu.au*

Electronic Supplementary Information pp. S1–S9 contains two tables (Tables S1 and S2) and eight figures (Figs. S1–S9).

Table S1 Characteristics of critical point dried CaAlg template beads and non-calcined hybrid template/TiO_2/ZrO_2 beads

Sample	Total weight loss (%)[a]	Total weight loss (%)[b]	Inorganic loading (%)[c]	BET surface area (m^2 g^{-1})	Pore size[d] (nm) (<30 nm)	$V_{mesopore}$[e] (cm^3 g^{-1}) (2–30 nm)	$V_{meso-macropore}$[f] (cm^3 g^{-1}) (30–300 nm)
Template							
TBrt	–	–	–	400 ± 1	–	0.401	0.732
TB50	–	–	–	522 ± 1	–	0.508	1.376
TB85	–	–	–	406 ± 1	–	0.411	0.773
$TBLN_2$	–	–	–	377 ± 1	–	0.458	1.381
Non-calcined sample							
TiZr[g]	32.2	–	67.8	335 ± 5	<2	0.161	0.129
Method A							
TiZr-TB50	35.2	–	64.8	339 ± 32	<2	0.165	0.138
TiZr-TB85	39.9	–	60.1	285 ± 10	<2	0.165	0.121
TiZr-$TBLN_2$	19.9	–	80.1	368 ± 2	<2	0.124	0.058
Method B							
TiZr-ST-100	30.9	10.8	58.3	359 ± 1	<2	0.162	0.255
TiZr-ST-140	23.9	17.2	58.9	359 ± 2	<2, 8.8 ± 0.1	0.236	0.296
TiZr-ST-180	19.4	19.6	61.0	328 ± 2	<2, 11.0 ± 0.1	0.280	0.300
TiZr-ST-240	12.6	22.8	64.6	204 ± 1	<3, 20.2 ± 0.6	0.288	0.352
TiZr-ST-NH_3-100	32.2	10.2	57.6	351 ± 4	<2	0.170	0.157
TiZr-ST-NH_3-140	20.9	17.5	61.6	365 ± 1	<2, 9.6 ± 0.1	0.269	0.271
TiZr-ST-NH_3-180	17.2	20.5	62.3	317 ± 1	<2, 12.3 ± 0.1	0.294	0.301
TiZr-ST-NH_3-240	10.6	24.0	65.4	194 ± 2	<3, 21.0 ± 0.4	0.284	0.354

[a]Determined from TGA in the temperature range of 25–500 °C.
[b]Estimated from the difference between the weight of the dry beads before and after solvothermal treatment. Assuming that total weight loss incurred is only related to weight of organic decomposed during solvothermal treatment.
[c]Estimated from the following calculation: 100% − sum of weight loss incurred during solvothermal treatment and weight loss determined from TGA.
[d]Average mesopore size obtained from three separate measurements within a size range of 2–30 nm through BJH analysis of the N_2 adsorption branch.
[e,f]Obtained from BJH analysis of the N_2 adsorption branch within the specified mesopore/meso-macropore size range.
[g]Reference bead sample prepared using template beads conditioned at room temperature and in the absence of a solvothermal treatment.

Table S2 Langmuir AO7 adsorption capacities and associated constants obtained for the corresponding non-solvothermally and solvothermally treated TiO_2/ZrO_2 in the absence and presence of NH_3

Sample	q_{max} (mg g^{-1})	b	R^2
TiZr-500	40 ± 3	0.20 ± 0.10	0.922
TiZr-ST-100	47 ± 2	0.15 ± 0.04	0.976
TiZr-ST-140	74 ± 4	0.17 ± 0.04	0.976
TiZr-ST-180	92 ± 4	0.10 ± 0.02	0.983
TiZr-ST-NH_3-100	50 ± 3	0.05 ± 0.02	0.968
TiZr-ST-NH_3-140	85 ± 6	0.11 ± 0.04	0.964
TiZr-ST-NH_3-180	101 ± 5	0.12 ± 0.03	0.978

$[AO7]_{initial}$ = 25–300 ppm, pH = 2.01, [beads] = 1 g L^{-1}.

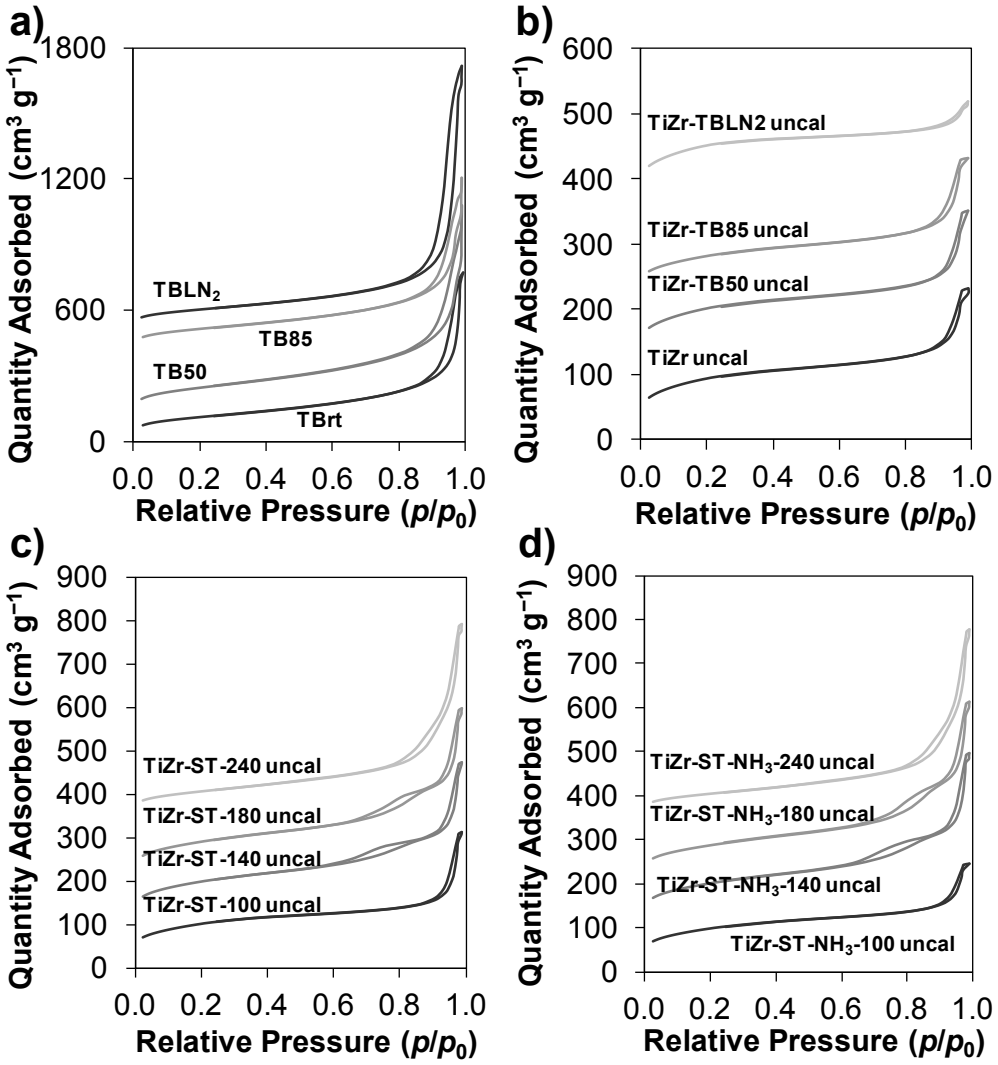

Fig. S1. (a) N_2 sorption isotherms of critical point dried CaAlg beads conditioned at room temperature (TBrt), 50 °C (TB50), 85 °C (TB85), and −196 °C (liquid N_2; $TBLN_2$); for clarity, isotherms are offset by +0, +100, +400, and +500, respectively, along the *y*-axis. N_2 sorption isotherms of non-calcined hybrid template/TiO_2/ZrO_2 beads prepared from (b) Method A, using template beads conditioned at varying temperatures (including room temperature – TiZr uncal); and (c,d) Method B (solvothermal treatment) in the absence and presence of NH_3, respectively, at varying temperatures; for clarity, all isotherms are offset in the order from bottom to top by +0, +100, +200, and +350 along the *y*-axis.

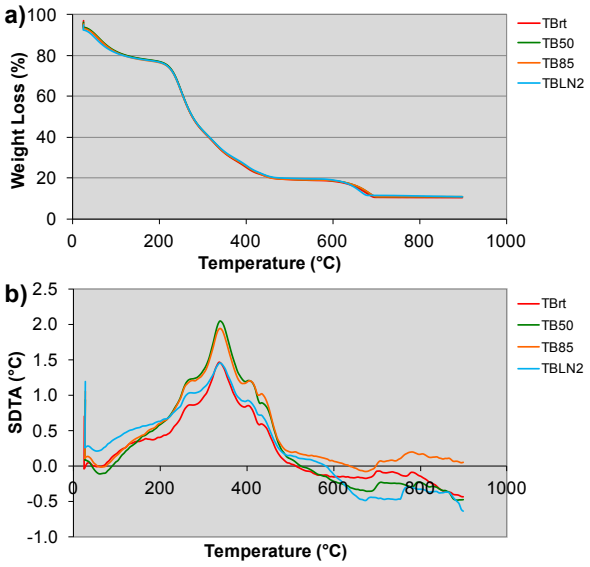

Fig. S2. (a) Thermograms and (b) single differential temperature (SDTA) profiles of critical point dried CaAlg template beads conditioned at room temperature (TBrt), 50 °C (TB50), 85 °C (TB85), and −196 °C (liquid N_2; $TBLN_2$).

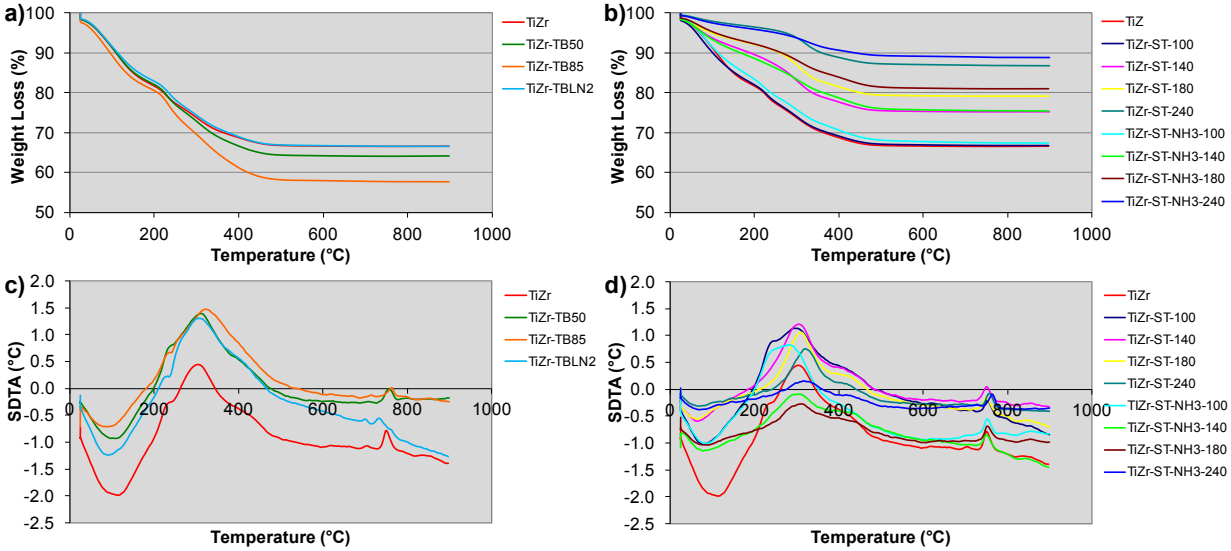

Fig. S3. Thermograms of non-calcined hybrid template/TiO_2/ZrO_2 beads produced from (a) Method A, using template beads conditioned at varying temperatures (including room temperature – TiZr); and (b) Method B (solvothermal treatment) in the absence and presence of NH_3 at varying temperatures. Single differential temperature (SDTA) profiles of non-calcined hybrid template/TiO_2/ZrO_2 beads produced from (c) Method A and (d) Method B.

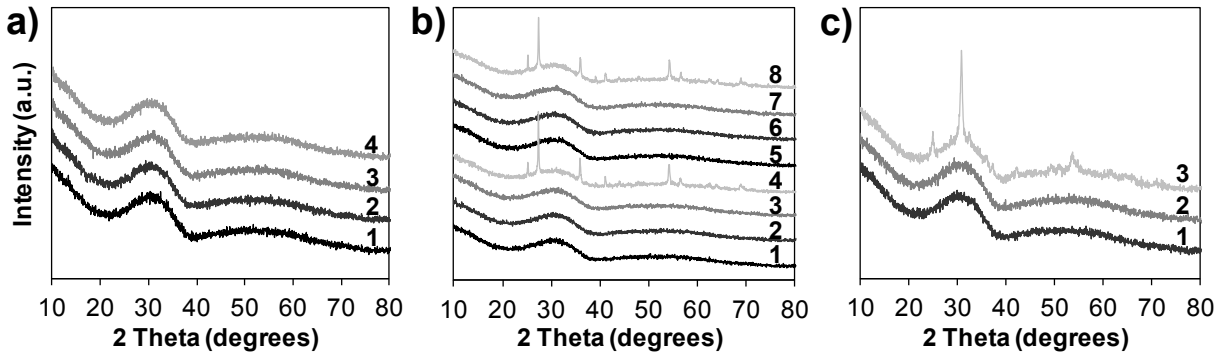

Fig. S4. XRD patterns of TiO_2/ZrO_2 beads produced from (a) Method A: template beads conditioned at (1) room temperature, (2) 50, (3) 85, and (4) −196 °C; (b) Method B: hybrid beads subjected to solvothermal treatment in the absence of NH_3 at (1) 100, (2) 140, (3) 180, and (4) 240 °C, and in the presence of NH_3 at (5) 100, (6) 140, (7) 180, and (8) 240 °C; and (c) Method C: hybrid beads calcined at varying temperatures of (1) 500, (2) 600, and (3) 700 °C.

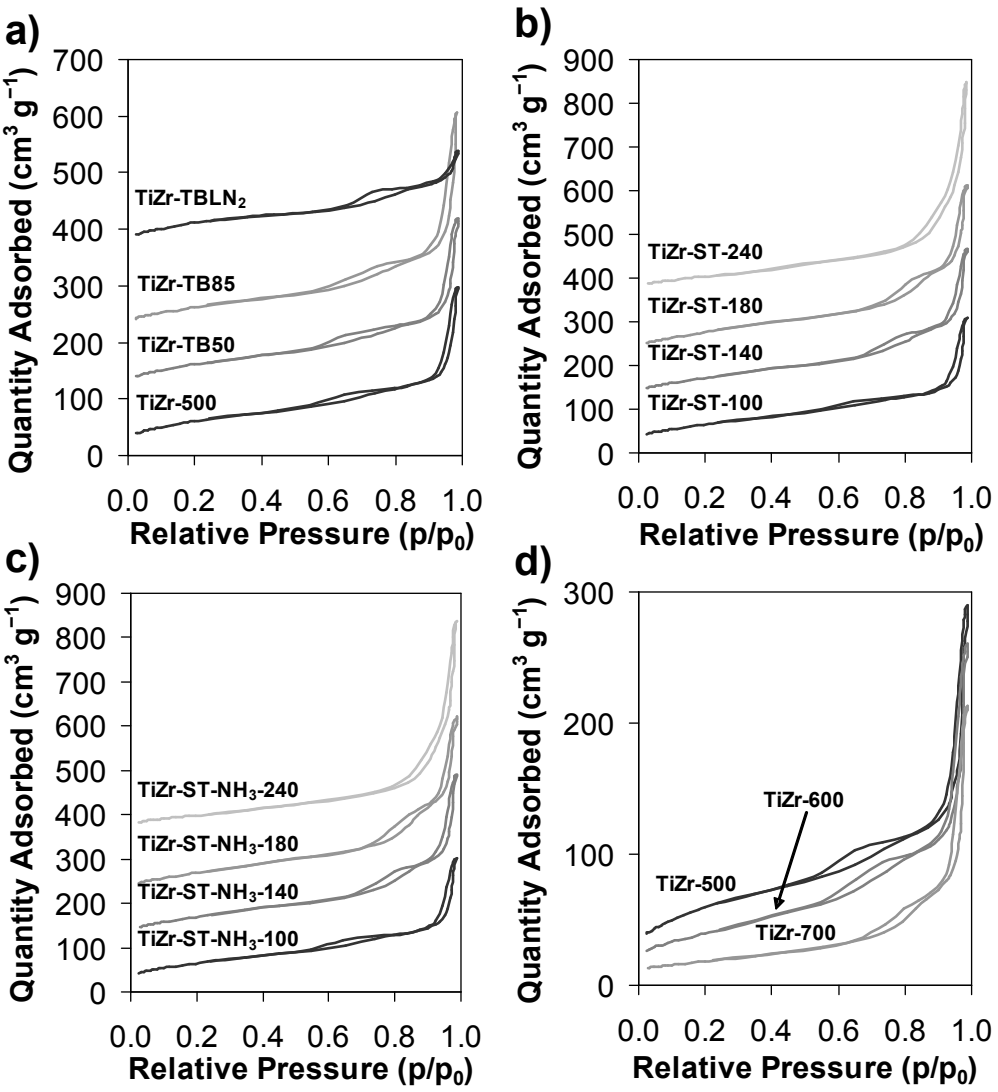

Fig. S5. N_2 sorption isotherms of TiO_2/ZrO_2 beads produced from (a) Method A, using template beads conditioned at varying temperatures (including room temperature – TiZr-500); (b,c) Method B (solvothermal treatment) in the absence and presence of NH_3, respectively, at varying temperatures; and (d) Method C, at varying calcination temperatures. For clarity, all isotherms are offset in the order from bottom to top by +0, +100, +200, and +350 along the *y*-axis except for the isotherms in (d) where no offset holds.

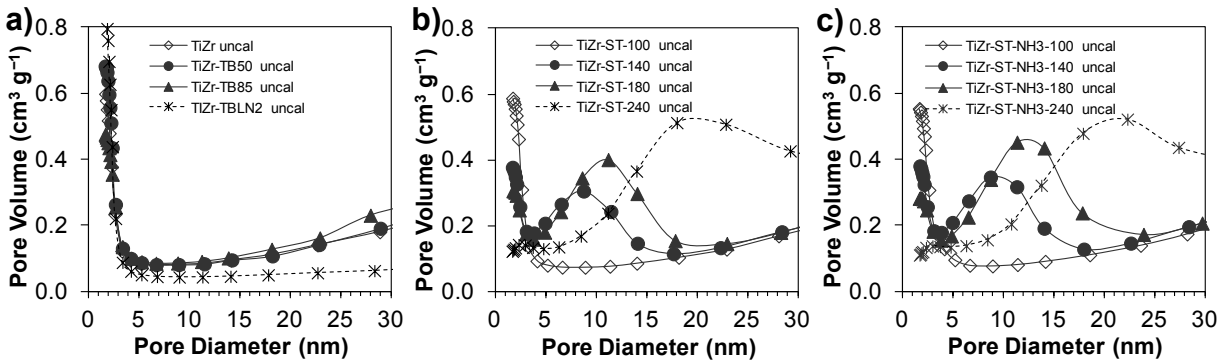

Fig. S6. Pore size distributions (<30 nm) determined from BJH analysis of the N_2 adsorption branch on non-calcined hybrid template/TiO_2/ZrO_2 beads prepared from (a) Method A, using template beads conditioned at varying temperatures (including room temperature – TiZr uncal); and (b,c) Method B in the absence and presence of NH_3, respectively, at varying temperatures.

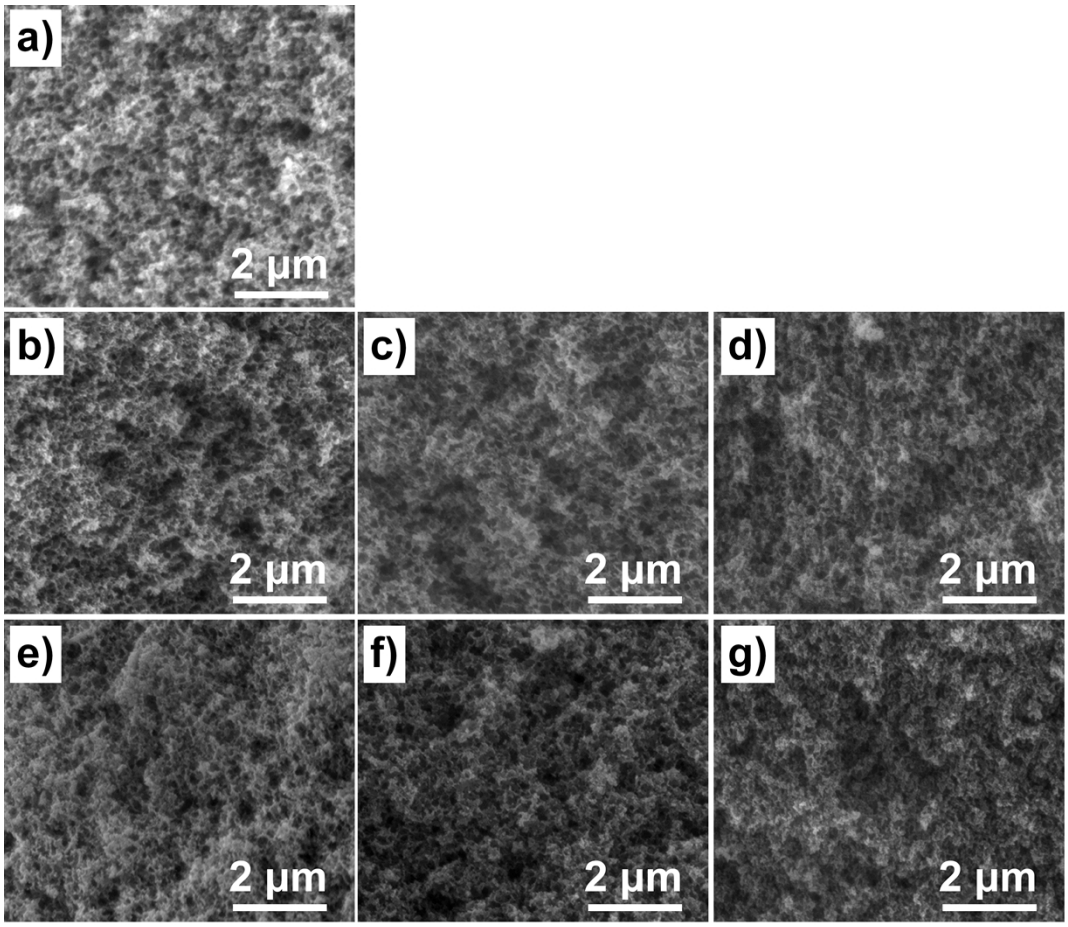

Fig. S7. Low-magnification SEM images of (a) non-solvothermally treated sample (TiZr-500) and solvothermally treated TiO_2/ZrO_2 beads in the absence of NH_3 at (b) 100, (c) 140, and (d) 180 °C, and presence of NH_3 at (e) 100, (f) 140, and (g) 180 °C.

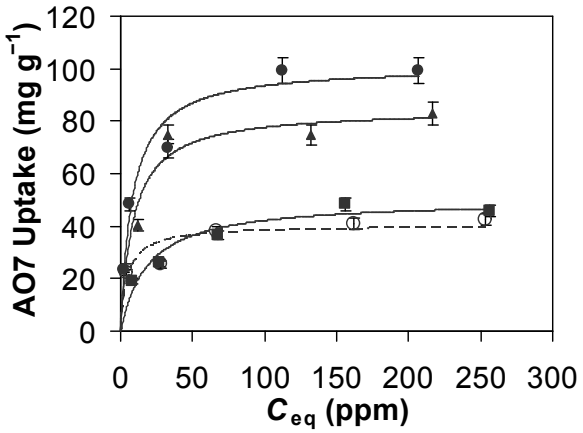

Fig. S8. AO7 uptake adsorption isotherms of (☒) non-solvothermally treated sample (TiZr-500) and solvothermally treated samples in the presence of NH_3 at (●) 100, (■) 140, and (⌀) 180 °C. The broken and solid lines correspond to Langmuir fits for the four respective samples. $[AO7]_{initial}$ = 25–300 ppm, pH 2.01, [beads] = 1 g L^{-1}.

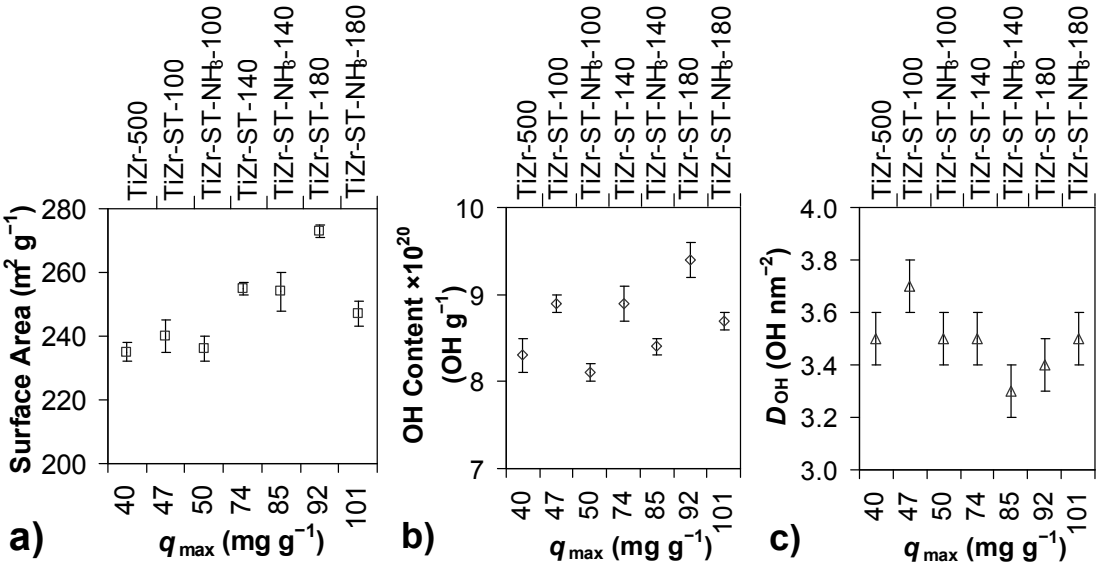

Fig. S9. Dependency of (a) surface area, (b) hydroxyl content (OH g^{-1}), and (c) hydroxyl density (D_{OH}) on AO7 adsorption capacity (q_{max}) obtained for the non-solvothermally treated sample (TiZr-500) and solvothermally treated samples at varying temperatures in the absence and presence of NH_3.